Assessing the effect of long-term formalin preservation on zooplankton biovolume estimates

by

Nicole Fung

A thesis submitted in partial fulfilment of the requirements of

Honours in Biology

at

University of Victoria

Supervisor:

Dr. John Dower

University of Victoria

ABSTRACT

Energy and carbon transfer from phytoplankton to fish is regulated by zooplankton in marine systems, acting as a link to higher trophic levels and exporting carbon to deeper waters. To determine the relative magnitude of these processes, the biomass and biometrics of zooplankton are often studied. Biomass is generally estimated based on wet mass, dry mass, or carbon mass; however these methods involve a destructive method, ceasing possibilities of future analysis of samples. The alternative method of estimating biomass via measuring biovolume (BV) through image-analysis provides a permanent electronic record of samples. Though an issue with this method is shrinkage observed in formalin-preserved zooplankton, which would provide an underestimated biomass. Therefore, this study investigates the response of different zooplankton taxa when preserved in formalin to determine taxa-specific conversion factors that can provide the means for more accurate biomass estimates. By tracking biovolume changes of different taxa over a two-month period and comparing percent biovolume of taxa in their fresh and preserved state, it was determined that taxa shrink at different rates and by different amounts. Copepods (and specifically *Eucalanus* sp.), decapod megalops, euphausiids, small hyperiids (BV < 60 mm^3), and gastropod veliger larvae had statistically significant differences in the fresh and preserved percent biovolume. Additionally, the acquired conversion factors for several taxa can now be used to correct for the underestimated biovolumes obtained through image-analysis, as a proxy for biomass. This highlights the bias in estimates from previous applications that have investigated ecosystem energy flow or determined how biomass changes in differing oceanographic conditions. While this method has advantages, it is limited to a coarser taxonomic resolution of samples than what could be accomplished with microscopic analysis. Future work could include more taxa to obtain more conversion factors and higher sample size of taxa for more accurate conversion factors.

Table of Contents

Abstract ii

Table of Contents iii

List of Figures iv

List of Tables vi

Introduction 1

Methods 4

Results 8

Discussion 14

Acknowledgements 18

References 19

Supplementary Data 22

List of Figures

Figure 1. A 60 cm diameter bongo net with 250 µm mesh (a) and a 1000 µm mesh Tucker trawl (b). Photo credits of (a) to Woods Hole Oceanographic Institution and (b) to Nicolas Ens.

Figure 2. Visualized timeline of sample collection and scan frequency of samples as outlined in Table 1.

Figure 3. Steps in the scanning procedure after getting rinsed with freshwater through a 250µm mesh sieve and poured onto the scanbed (24.5 x 15.8 cm). a) separated zooplankton prepared to be scanned on the ZooScan. Examples of zooplankton vignettes from ZooScan; b) Decapod megalops, c) Copepoda, d) Sergestidae, e) Hyperiidae. Scale bars represent 2 mm.

Figure 4. A reference to the major and minor axis lengths of a copepod used to calculate biovolume.

Figure 5. Changes in percent (%) average biovolume of a) large copepods, b) *Eucalanus bungii*, c) large euphausiids, d) Hydromedusae, e) *Primno* sp., and f) Veliger larvae from a fresh state to after preservation in buffered formalin over 60 days. n indicates number of individuals present in the fresh sample. Figure is based on measurements of individuals in jars 1 and 2 where a full scan schedule was completed (Table 1). Curves indicate exponential shrinkage rates with the sample stabilizing well within two months.

Figure 6. Average percent biovolume (%) of a) large copepods, b) *Eucalanus bungii*, c) large euphausiids, d) Hydromedusae, e) *Primno* sp., and f) Veliger larvae before and after 60 days of preservation in buffered formalin, with the blue X indicating mean percent average biovolume. Plots are overlayed with individual data points. Note that the y-axis does not have the same scale on all plots.

Figure 7. Example of vignettes of the same *Primno* sp. individual (a,b) and *Euclanus* bungii (c, d) from a fresh sample and after preservation in buffered formalin for 60 days, *respectively*. Scale bars are of equal length across all four vignettes and represent 1 mm.

Figure A1. Euphausiid vignette with an estimated biovolume of 70.9407 mm^3 before correction and 12.1441 mm^3 after correction.

Figure A2. Scatterplot of biovolume (BV) against the major axis used to further divide hyperiid taxa into size categories. Example in figure shows distinct clusters of different sized hyperiids; large individuals defined as BV > 60 mm^3 and small individuals BV < 60 mm^3.

Figure A3. Examples of flipped-up carapaces of euphausiids after 58 days of preservation in buffered formalin solution.

List of Tables

Table 1. Scanning schedule of zooplankton samples.

Table 2. Taxa specific percent biovolumes (BV) of preserved samples (%) and their respective conversion factors (CF) after 60 days. Included are test statistics for t-tests (t) and Wilcoxon rank sum tests (W) with their respective p-values (******* indicates significant values with $p < 0.05$), as well as degrees of freedom (df) for taxa where a t-test was conducted.

Table 3. Taxa-specific shrinkage factors in the form of differences in the mean percent average biovolume (%) and median percent average biovolume (%) of fresh and preserved samples with standard error (%); positive mean and median differences indicate shrinkage. Number of fresh and preserved individuals (n) of each taxa and the interquartile range (IQR) of fresh and preserved samples (%) is also included.

INTRODUCTION

Importance of zooplankton

Zooplankton play a critical role in marine ecosystems as a link between primary producers and higher trophic levels (Dai *et al*., 2016) in their role as key prey for taxa including various fishes (including larval, juvenile and adult stages), marine mammals (particularly baleen whales) and many seabirds. They also play a key role in the biological pump, cycling nutrients throughout the water column and exporting organic carbon from the surface to the deep ocean. (Cornils *et al*., 2022; Nakamura *et al*., 2017). By understanding spatial and temporal patterns of zooplankton distribution and biomass in response to interannual variations, the success of higher trophic levels including fish can be better approximated based on their larval survivorship and growth (Cushing, 1990; Nakamura *et al*., 2017). Therefore, it is important to study biomass and biometrics of zooplankton to determine how much food and nutrients are available to higher trophic levels (Dai *et al*., 2016; Garijo & Hernández-León, 2015).

Measuring biomass via image analysis

Total zooplankton biomass is often used as a proxy for prey biomass to study how much energy is available to higher trophic levels (Davis *et al*., 2004). Upon collection, samples are often processed to determine wet mass, filtered and dried to determine dry mass, or carbon mass (McEnnulty *et al.*, 2020). However, these current methods of determining biomass via dry weight measurements provide little taxonomic resolution and involves a destructive method, making future taxonomic analysis impossible (Alcaraz *et al.*, 2003; Garijo & Hernández-León, 2015; Gislason & Silva, 2009). Instead, an alternative is to estimate biomass through biovolume measurements via image-analysis. The biomass of a zooplankton taxa can be linearly modelled from biovolume measurements, as determined by previous studies (Alcaraz *et al*., 2003; Garijo & Hernández-León, 2015; Hernández-León & Montero, 2006).

The development of digital imaging technology and machine learning has provided a new methodology for measurement of zooplankton biometrics. Imaging technology including Video Plankton Recorder (VPR), Underwater Vision Profiler (UVP), and Laser Optical Plankton Counter (LOPC) have enabled collection of optical in-situ data (Cornils *et al*., 2022; Davis *et al.*, 2004). However, for analysis of collected zooplankton samples, instruments such as the ZooScan provide a closer estimate of biomass because any detritus or non-living particles can be removed

prior to analysis (Cornils *et al.*, 2022). The Zooscan functions as a scanner for zooplankton samples, producing two dimensional vignettes of individual zooplankters ((Di Mauro *et al.*, 2011; Gorsky *et al.*, 2010). Blank background scans taken prior to scanning are subtracted from the raw image of the scan, and grey values are normalized to provide contrast of individual zooplankter vignettes (Gorsky *et al.*, 2010). Software like ZooProcess can then extract measurements such as the major and minor axis length from a vignette, which can then be used to calculate biovolume as a proxy for biomass (Gislason & Silva, 2009; Gorsky *et al.*, 2010). Additionally, these vignettes can be classified and sorted through machine learning algorithms followed by manual validation, providing a taxon-specific estimate of biomass. This allows for faster processing and analysis of zooplankton samples, reducing the large efforts required from high-resolution sampling that aim to resolve the patchiness of zooplankton (Davis *et al.*, 2004). Image analysis also allows for the biomass estimation of historical samples where biomass data may not have been collected or it can be used in conjunction with acoustic data to estimate the spatial distribution of zooplankton (Benfield *et al.*, 1998). This provides a taxonomically fine-grained alternative method to the traditional destructive dry mass and incineration of zooplankton samples for the estimation of biomass (Gislason & Silva, 2009; Gorsky *et al.*, 2010).

Shrinkage from formalin preservation

Biometric measurements are ideally performed using fresh unpreserved zooplankton. However, samples are rarely ever processed immediately after collection due to (i) logistical constraints (eg. equipment onboard the research vessel is inadequate or there is not sufficient time) and (ii) fresh zooplankton samples quickly degrade if left unpreserved. Rather, zooplankton samples are often preserved in a buffered formalin solution to maintain the integrity of the samples over a long period of time (Gifford *et al.*, 2000). Other fixatives such as ethanol and Lugol's iodine are also used, but are not normally recommended when estimating biomass due to more severe shrinkage and greater dry weight losses (Giguère *et al.*, 1989; Stoecker *et al.*¸1994). As zooplankton are preserved, however, they contract and shrink due to muscular contraction, water and lipid leaching, and reactions between formalin and various body tissues (Giguère *et al.*, 1989; Kapiris *et al.*¸1997; Omori, 1978; Stoecker *et al.*¸1994). This shrinkage of zooplankton affects biovolume measurements of preserved specimens when being analyzed via

image analysis, resulting in underestimated biomass (Kapiris *et al.*¸1997). The main reasons for shrinkage in zooplankton are from muscular contraction, water and lipid leaching, and the chemical reaction between formalin and their body. The degree to which these parameters have influence on the rate of shrinkage differs between the various developmental stages and sizes of zooplankton, as well as across the different taxa (Giguère *et al.*, 1989; Kapiris *et al.*¸1997). Species-specific morphologies such as body wall thickness and composition, as well as surface area of the body are also likely to play a factor in the rate of shrinkage. Ahlstrom & Thrailkill (1962), found that due to the exoskeleton of crustaceans, samples mainly composed of copepods, euphausiids, amphipods, or decapod larvae experienced the least amount of shrinkage. Meanwhile, samples mainly composed of jelly-like constituents including salps and medusae experienced the greatest amount of shrinkage (Thibault-Botha & Bowen, 2004). Additionally, small-sized individuals with high surface to volume ratios experience greater shrinkage as suggested by Thibault-Botha & Bowen (2004). Three other factors that can contribute to patterns of post-preservation shrinkage are (i) the temperature at which the zooplankton are stored, (ii) the formalin concentration of the preservative and (iii) the ratio of formalin:biomass in the sample jar, though these are often standardized in sample preservation and storage (Kapiris *et al.*¸1997; Omori, 1978).

Most previous studies have investigated shrinkage in only select species or bulk zooplankton samples, observing shrinkage in length of various body dimensions of zooplankton (Alcaraz *et al.*, 2003; Kapiris *et al.*, 1997; Lafontaine and Leggett, 1989; Stoecker *et al.*¸1994). This study aims to investigate how different zooplankton taxa respond to formalin preservation over time. By tracking the biovolume changes of different taxa of zooplankton, this will in turn provide the means to determine taxa-specific conversion factors that can be multiplied by the biovolumes of the zooplankton in their preserved state for the estimated in-situ biomass. These estimates can then be used to determine how much energy is available to higher trophic levels and the survival or growth of higher trophic levels can be better assessed based on the spatial and temporal variation in zooplankton.

METHODS

Sampling

Zooplankton samples were collected during a Fisheries and Oceans Canada survey on September 2nd and 3rd, 2022, along the west coast of Vancouver Island (WCVI) aboard the *CCGS Sir John Franklin* (50° 38.858 N, 129° 7.744 W and 48° 24.736 N, 124° 18.261 W, respectively). Two samples of zooplankton were collected via i) a vertical net haul using a 60 cm diameter bongo net with a 250 µm mesh to 178 m and ii) an oblique tow using a 1000 µm mesh Tucker trawl to 750 m (Figure 1). Upon collection, fresh samples were narcotized using isotonic magnesium chloride ($MgCl_2$) and kept refrigerated before the scanning procedure.

Figure 1. A 60 cm diameter bongo net with 250 µm mesh (a) and a 1000 µm mesh Tucker trawl (b). Photo credits of (a) to Woods Hole Oceanographic Institution and (b) to Nicolas Ens.

ZooScan Procedure

Intact zooplankton from the Tucker trawl samples were hand-picked two days after collection (i.e. to ensure no empty carapaces or individuals with damaged body walls contaminated the samples) and then split using a Folsom splitter to a fraction of ¼ and stored in four separate jars. Euphausiids and chaetognaths from the bongo net were also handpicked from the bulk samples. Handpicked samples were immediately scanned using a Zooscan© v2 scanner prior to preservation, then preserved in a 10% borax-buffered formalin solution and scanned

again 1 hr after preservation. To track changes in percent biovolume, these same samples were repeatedly scanned over a two-month period, the timeframe over which previous studies have found that all or most species in a sample will have stabilized (Kapiris et al.¸1997; Lafontaine and Leggett, 1989). During the first week after collection, samples were scanned daily, followed by one scan every three days until day 16. From day 17 to 30 after sample collection, scans were conducted every seven days, and beyond day 30 after collection, scans were conducted every fourteen days until day 60, when scanning procedures ended (Table 1). In all, 15 scans of each sample were collected over the 60 days (Table 1, Figure 2).

Table 1. Scanning schedule of zooplankton samples.

Days post preservation	Scan frequency	Total scans (in time period)
0 (Fresh)	1	1
1-7	1 scan/day	7
8-16	1 scan/ 3 days	3
17-30	1 scan/ 7 days	2
30+	1 scan/14 days	2
60	END	

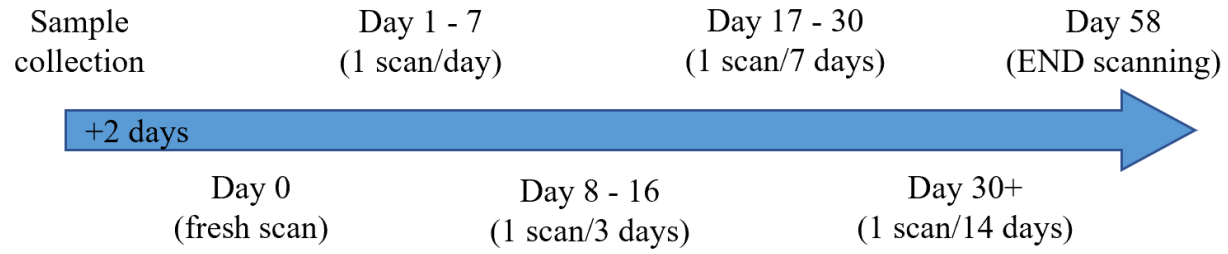

Figure 2. Visualized timeline of sample collection and scan frequency of samples as outlined in Table 1.

The ZooScan scanning procedure followed that of Gorsky *et al.* (2010), however samples were not size fractionated prior to scanning. In brief, the procedure was as follows: to normalize gray values of the sample scan image, two background scans were taken prior to scanning each day. The sample was then rinsed with fresh water through a 250µm mesh sieve and poured onto

the scanbed where individuals were separated by hand (Figure 3a). The sample was then scanned and processed using Zooscan and Zooprocess (Gorsky *et al.*, 2010) to obtain scanned vignettes of individual zooplankton (Figure 3b-e). Vignettes containing more than one individual were then separated manually. Plankton Identifier software (Version 1.3.4; Gasparini, 2013) was then used to create a learning set of images that distinguished the vignettes into different taxa including Copepoda (excluding *Eucalanus sp.*), *Cyphocaris* sp., decapod megalops, *Eucalanus* sp., Euphausiidae, Hydromedusae, Hyperiidae (excluding *Primno* sp.), *Primno* sp., Sergestidae, and gastropod veliger larvae. The selected taxa had a sample size ≥ 4 in either the fresh or preserved state, deemed to be sufficient for further analysis. Taxa were categorized to the furthest level of identification possible through vignettes. Taxa that were algorithmically determined through the learning set were then validated manually.

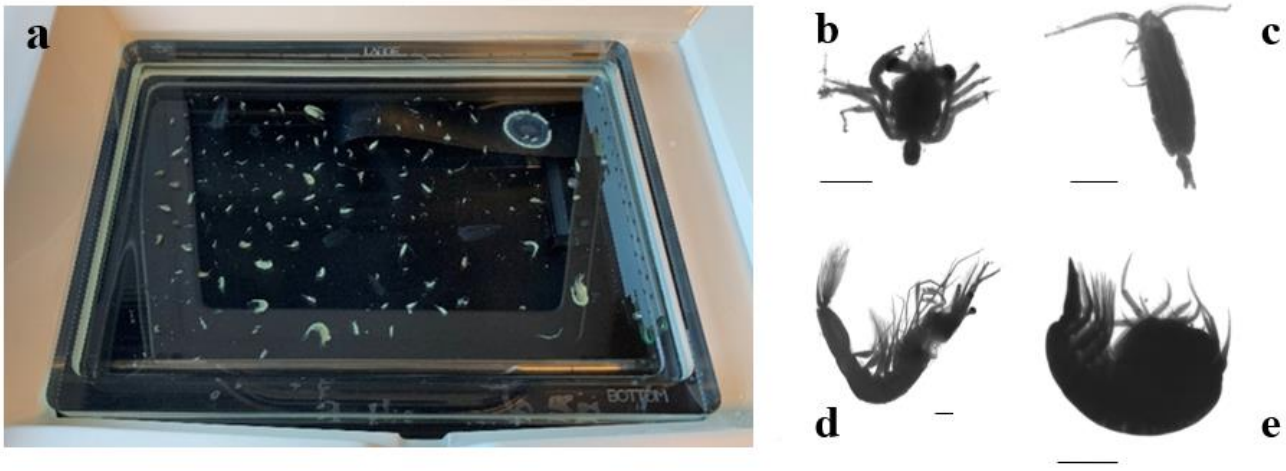

Figure 3. Steps in the scanning procedure after getting rinsed with freshwater through a 250µm mesh sieve and poured onto the scanbed (24.5 x 15.8 cm). a) separated zooplankton prepared to be scanned on the ZooScan. Examples of zooplankton vignettes from ZooScan; b) Decapod megalops, c) Copepoda, d) Sergestidae, e) Hyperiidae. Scale bars represent 2 mm.

Data Analysis

The Zooprocess software calculates the major and minor axis lengths of an ovoid of equivalent area to each individual zooplankter (Figure 4). With a pixel correction constant

(Garcia-Comas, 2010), the biovolume (BV) of the selected vignette was then calculated via R (Version 4.2.2) using the following equation modified from Dai *et al.* (2016):

$$BV = 4\pi/3 * (major/2) * (minor/2)^2 * 0.0105833^3 \quad \text{(Eqn. 1)}$$

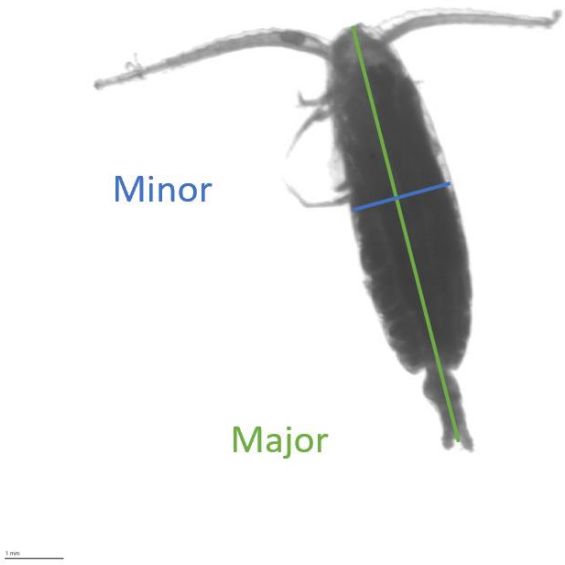

Figure 4. A reference to the major and minor axis lengths of a copepod used to calculate biovolume.

It was noted during scanning that due to the curvature of euphausiids and the silhouette of the pleopods, the ellipsoidal biovolume estimation overestimates the biovolume of euphausiids (Supplementary data, Figure A1). To compare how much the biovolume was overestimated, the curve length of the euphausiid from the middle of the eye to the end of the telson was calculated using FishSizer V3.0 (Rasmussen *et al.*, 2022). After comparing, the BV calculation for euphausiids was corrected using the following equation:

$$BV_{Euphausiidae} = e^{0.58586 * \ln(BV)} \quad \text{(Eqn. 2)}$$

In order to provide a more comprehensive comparison of shrinkage within different taxa, additional exploration with plots of major against minor axis or major axis against biovolume were used to subcategorize taxa. Taxa were further divided into size categories if they had

distinct clusters across samples (Supplementary data, Figure A2), which included copepods, euphausiids, and hyperiids. Average shrinkage factor of each taxonomic group was then calculated, with the average unpreserved biovolume of each taxon being scaled as one hundred percent:

$$SF_t = (BV_t / \overline{BV_0}) * 100\% \quad \text{(Eqn. 3)}$$

Where SF_t is the shrinkage factor at day t expressed as a percent of the ratio of biovolume at day t (BV_t) to the taxon average unpreserved biovolume ($\overline{BV_0}$). The conversion factor (CF) for each taxon was calculated through the reciprocal of the average percent biovolume of preserved samples ($SF_{preserved}$):

$$CF = 100\% / SF_{preserved} \quad \text{(Eqn. 4)}$$

Outliers observed from plotting percent average BV against scan day were manually cross-referenced with their respective vignettes and examined for unusual configurations or missing limbs. If so, vignettes were manually removed from the scanning procedure and not included in further analysis. Both mean and median differences between fresh and preserved percent biovolume were examined due to the data being inherently positively skewed. Significance of differences between fresh and preserved samples were tested via t-tests and Wilcoxon rank sum tests for normal and non-normal taxa, respectively.

RESULTS

Most taxa, except for small euphausiids, showed a similar pattern of exponential shrinkage after preservation in formalin. In general, most of the shrinkage occurred in the first few days after preservation, before stabilizing after 10 - 45 days (Figure 5). However, different taxa shrank at different rates and by different amounts, as indicated by differences in average percent biovolume in the preserved state after stabilization (Figure 6 and 7, Tables 2 and 3). Taxa that had significantly different average percent biovolumes in their fresh versus preserved states included: copepods of all size categories (large, medium, small), decapod megalops, the copepod *Eucalanus bungii*, both large and small euphausiids, small hyperiid amphipods, and veliger larvae (Table 2).

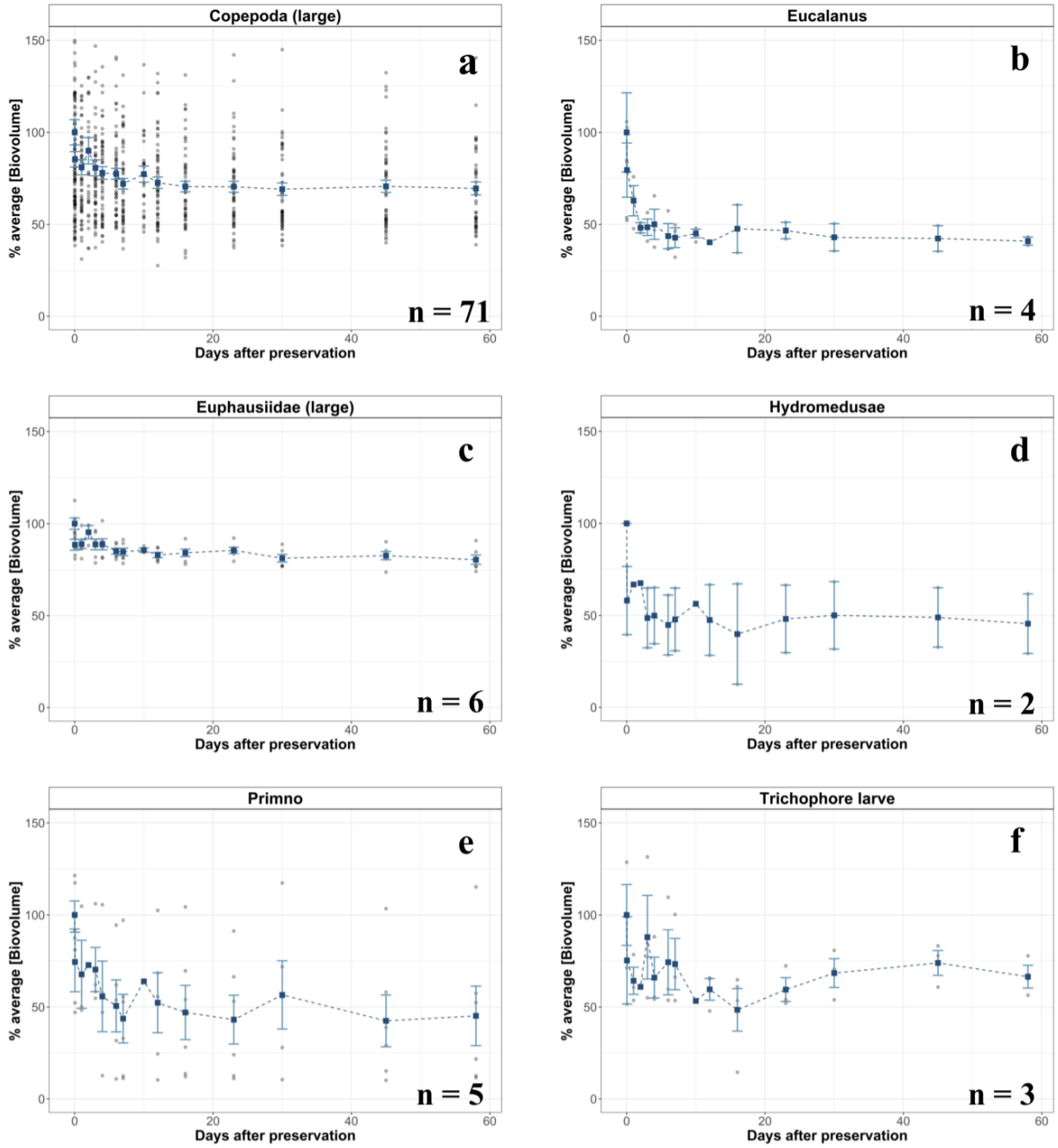

Figure 5. Changes in percent (%) average biovolume of a) large copepods, b) *Eucalanus bungii*, c) large euphausiids, d) Hydromedusae, e) *Primno* sp., and f) Veliger larvae from a fresh state to after preservation in buffered formalin over 60 days. n indicates number of individuals present in the fresh sample. Figure is based on measurements of individuals in jars 1 and 2 where a full scan schedule was completed (Table 1). Curves indicate exponential shrinkage rates with the sample stabilizing well within two months.

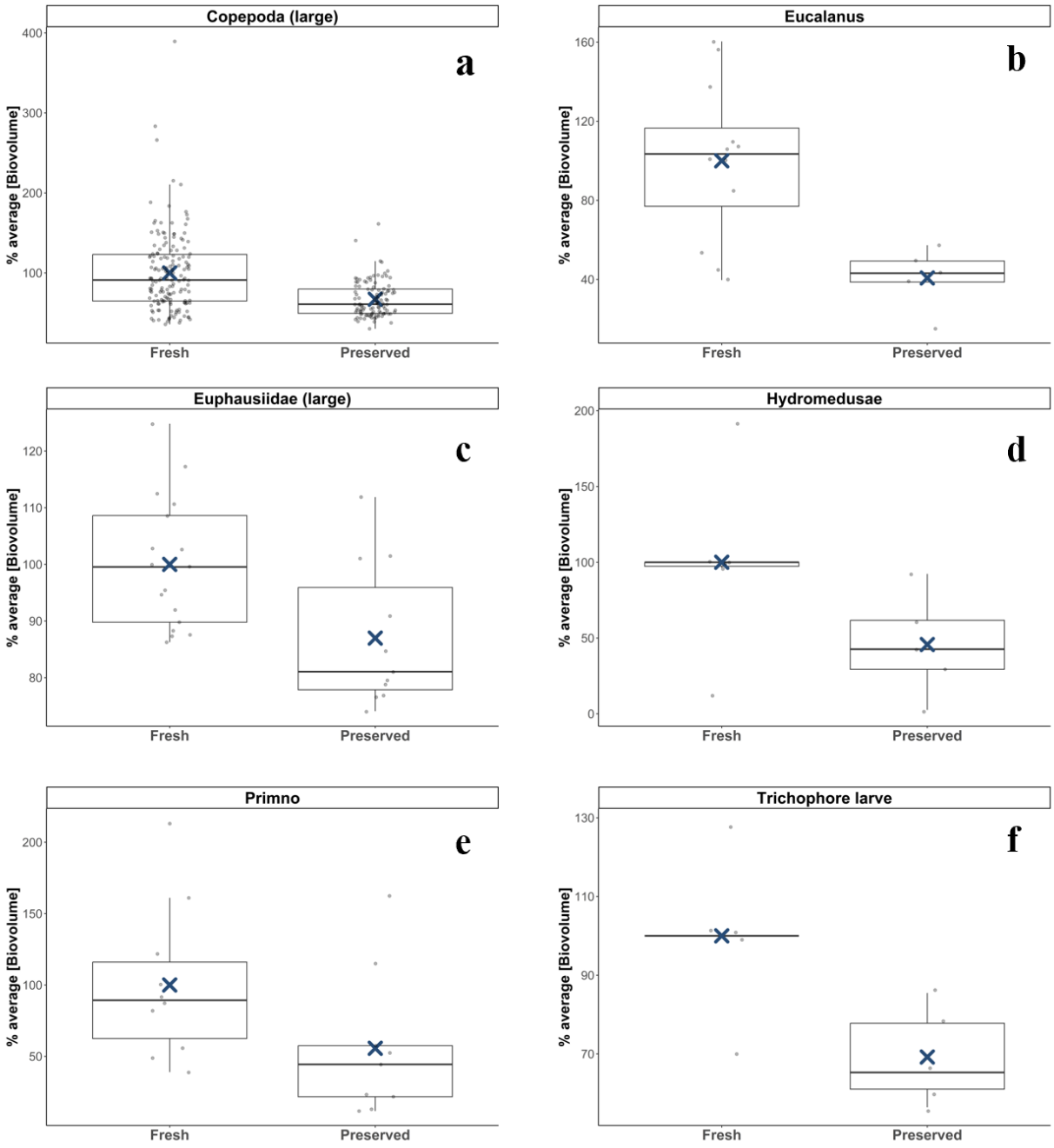

Figure 6. Average percent biovolume (%) of a) large copepods, b) *Eucalanus bungii*, c) large euphausiids, d) Hydromedusae, e) *Primno* sp., and f) Veliger larvae before and after 60 days of preservation in buffered formalin, with the blue X indicating mean percent average biovolume. Plots are overlayed with individual data points. Note that the y-axis does not have the same scale on all plots.

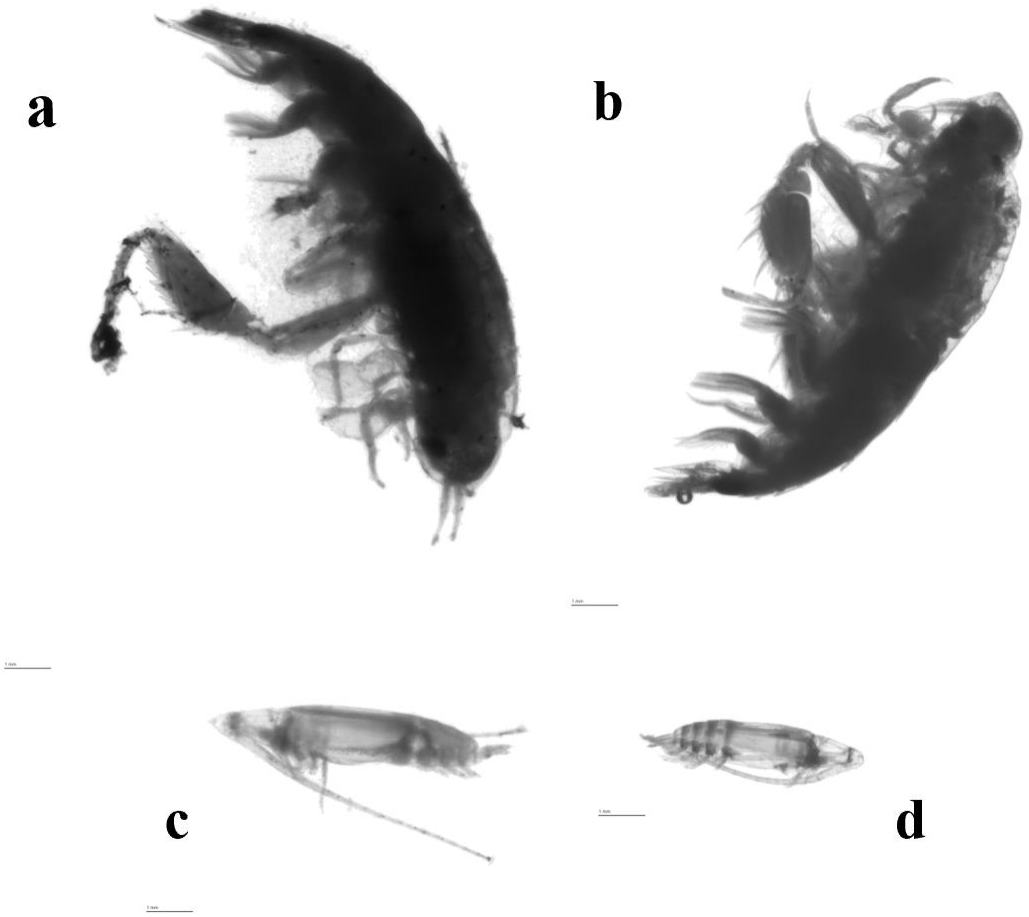

Figure 7. Example of vignettes of the same *Primno* sp. individual (a,b) and *Euclanus* bungii (c, d) from a fresh sample and after preservation in buffered formalin for 60 days, *respectively*. Scale bars are of equal length across all four vignettes and represent 1 mm.

Within the three copepod groupings, there was a trend for the largest individuals (area >8 mm^2) to show the greatest amount of shrinkage ($BV_{preserved}$ = 67.092% BV_{fresh}), followed by medium copepods (8 mm^2 > area > 1.5 mm^2) (80.558%), and small copepods (area < 1.5 mm^2) with extremely minimal shrinkage (99.679%) (Table 2). Similarly with euphausiids, the larger individuals (BV > 25.5 mm^3) also had greater shrinkage (86.985%) than the smaller individuals (BV < 11 mm^3) that had higher percent biovolume after preservation (102.274%). Unlike the copepods and euphausiids, the size trend among the hyperiids was opposite with larger individuals (BV > 60 mm^3) demonstrating less shrinkage (98.337%) than small individuals (BV < 60 mm^3) (76.578%). (Table 2 and 3). Overall, the greatest shrinkage was observed within

Eucalanus bungii, with the lowest preserved percent biovolume and the highest conversion factor (40.739%; 2.455) (Table 2). This was followed by Hydromedusae which also demonstrated considerable shrinkage (45.716%), although not statistically significant (Table 2 and 3). Both *Eucalanus bungii* and Hydromedusae had conversion factors greater than 2, indicating underestimation of percent biovolume by more than two-fold. Decapod megalops and veliger larvae had statistically significant shrinkage with preserved percent biovolumes being 62.863% and 69.206%, respectively. Although not statistically significant, *Primno,* Sergestidae, and Cyphocaris also displayed shrinkage in descending order (their preserved percent biovolumes being 55.665%, 73.756%, 89.678% of fresh biovolumes, respectively).

Table 2. Taxa specific percent biovolumes (BV) of preserved samples (%) and their respective conversion factors (CF) after 60 days. Included are test statistics for t-tests (t) and Wilcoxon rank sum tests (W) with their respective p-values (******* indicates significant values with $p < 0.05$), as well as degrees of freedom (df) for taxa where a t-test was conducted.

				Test Statistic		
Taxa	**Preserved %BV**	**CF**	**df**	**t**	**W**	**p-value**
Copepoda (large)	67.092	1.490	-		35245	<0.001 ***
Copepoda (medium)	80.558	1.241	-		82215	<0.001 ***
Copepoda (small)	99.679	1.003	-		29646	<0.001 ***
Cyphocaris	89.678	1.115	9	0.354		0.732
Decapod megalops	62.863	1.591	-		55	<0.001 ***
Eucalanus	40.739	2.455	15	3.177		0.006 ***
Euphausiidae (large)	86.985	1.150	26	2.816		0.009 ***
Euphausiidae (small)	102.274	0.978	-		15931	<0.001 ***
Hydromedusae	45.716	2.187	9	1.871		0.094
Hyperiidae (large)	98.337	1.017	8	0.105		0.919
Hyperiidae (small)	76.578	1.306	-		17205	<0.001 ***
Primno	55.665	1.796	17	1.836		0.084
Sergestidae	73.756	1.356	10	1.124		0.287
Veliger larvae	69.206	1.445	8	2.920		0.019 ***

Table 3. Taxa-specific shrinkage factors in the form of differences in the mean percent average biovolume (%) and median percent average biovolume (%) of fresh and preserved samples with standard error (%); positive mean and median differences indicate shrinkage. Number of fresh and preserved individuals (n) of each taxa and the interquartile range (IQR) of fresh and preserved samples (%) is also included.

	n (individuals)		Difference (%)		IQR (%)		
Taxa	**Fresh**	**Preserved**	**Mean**	**Median**	**Fresh**	**Preserved**	**SE (%)**
Copepoda (large)	158	107	32.908	30.214	58.313	30.299	3.12
Copepoda (medium)	195	210	19.442	20.937	65.636	48.378	2.585
Copepoda (small)	135	108	0.321	-1.464	70.004	69.73	3.993
Cyphocaris	6	5	10.322	25.025	28.366	61.153	6.6
Decapod megalops	6	4	37.137	18.828	52.31	22.501	8.898
Eucalanus	12	5	59.261	60.304	39.545	10.657	6.121
Euphausiidae (large)	50	32	13.015	18.486	18.834	18.059	2.646
Euphausiidae (small)	17	11	-2.274	-2.260	70.182	51.719	2.941
Hydromedusae	6	5	54.284	57.363	2.627	32.349	6.873
Hyperiidae (large)	6	4	1.663	4.987	11.904	21.884	5.049
Hyperiidae (small)	99	86	23.422	23.955	86.639	61.321	3.692
Primno	10	9	44.335	44.903	53.563	35.758	5.898
Sergestidae	6	6	26.244	22.832	21.332	33.097	5.935
Veliger larvae	5	5	30.794	34.722	0	16.742	4.07

DISCUSSION

Current methods of determining zooplankton biomass involve filtering and drying of samples to determine dry weight but provide coarse taxonomic resolution and involve a destructive method (Garijo & Hernández-León, 2015). Recent technology has instead enabled biovolume measurements to be collected via image analysis, as a proxy for biomass estimates (Dai *et al.*, 2016; Davis *et al.*, 2004; Di Mauro *et al*., 2011; McEnnulty *et al.*, 2020). However, for logistical reasons, biometric measurements of zooplankton are usually made using preserved samples where zooplankters have shown evidence of shrinkage. This results in underestimated biomass estimates (Giguère *et al.*, 1989; Kapiris *et al.*, 1997). It has been noted that different

species of zooplankton shrink at different rates depending on their size and species-specific morphologies (Ahlstrom & Thraikill, 1962; Thubault-Botha & Bowen, 2003). Although previous studies have investigated shrinkage in select species or bulk zooplankton samples (Alcaraz *et al*., 2003; Kapiris *et al.*, 1997; Lafontaine and Leggett, 1989), to date no studies have investigated taxa-specific response of long-term formalin preservation for mixed zooplankton assemblages. This present work enables more accurate biomass estimates through image analysis, a non-destructive method that can provide higher taxonomic resolution, with taxa-specific conversion factors accounting for shrinkage after preservation.

As expected, the various taxa analyzed displayed different shrinkage rates due to their species-specific morphologies, with a general trend for crustacean zooplankton to display less shrinkage than soft-bodies or gelatinous zooplankton (Table 2). Crustacean zooplankton comprising of copepods, decapod megalops, euphausiids, and small hyperiids had significantly lower percent biovolume in their preserved state. Other crustacean zooplankton including *Cyphocaris* sp., large hyperiids, *Primno* sp., and sergestids also exhibited shrinkage, although not to a level that was statistically significant. Meanwhile, jelly-like zooplankton including Hydromedusae exhibited much greater shrinkage than that of crustacean zooplankton, with a preserved percent biovolume more than two times smaller than in the fresh state (Table 2). These findings are not unexpected, as there is evidence that crustacean zooplankton with an exoskeleton or hard-shell covering experience less shrinkage (Ahlstrom & Thrailkill, 1962; Devi, 1972; Põllupüü, 2007). Jelly-like zooplankton with greater water content and no hard covering, like hydromedusae, experience greater shrinkage due to the availability of water that can be leached out when preserved in formalin (Thibault-Botha & Bowen, 2004). Interestingly, copepods of the genus *Eucalanus* also experienced shrinkage to less than half their fresh biovolume (Table 2), similar to the Hydromedusae. This may be due to the low organic matter and high-water content of *Eucalanus* sp compared to other Copepoda species (Cass & Daly, 2015; Nakamura *et al.*¸ 2017). *Eucalanus* has been previously described as having a similar chemical composition to gelatinous zooplankton taxa (Nakamura *et al.*¸ 2017), with a greater availability of water that can be leached after preservation in formalin, possibly explaining a similar shrinkage rate to that of Hydromedusae (Table 2).

It has previously been suggested that smaller zooplankton, with a higher surface area to volume ratio, should experience greater shrinkage (Thibault-Botha & Bowen, 2004). In the

present study, however, among the taxa that were further divided into size categories, this was only true for hyperiids, with the smaller individuals experiencing greater shrinkage (Table 2). For both copepods and euphausiids, the larger individuals showed greater shrinkage, contrasting with suggestions of Thibault-Botha & Bowen (2004). This suggests that the availability of lipids or water available to be leached out has a greater effect than surface area to volume ratio when considering shrinkage in copepods and euphausiids. Although smaller individuals do have a higher surface area to volume ratio, once all their available lipid and water content has been leached out, there will be no more noticeable shrinkage. However, larger individuals often have greater reserves of lipids (Mayzaud *et al.*, 2003; Nakamura *et al.*, 2017), which have the potential to be leached out, resulting in greater shrinkage. Meanwhile, hyperiids often have lower lipid content than copepods and euphausiids (Wolowicz & Szaniawska, 1986) and thus unlike the shrinkage observed in euphausiids and copepods; smaller individuals shrank more than large individuals. Based on these observations, high availability of water or lipid content has greater influence on leaching effects compared to the surface area to volume ratio. However, when there is low availability of water or lipid content, the surface area to volume ratio has greater influence on leaching effects.

Despite different taxa having different shrinkage rates, all taxa showed a similar pattern of exponential shrinkage, with the greatest amount of shrinkage occurring in the first few days post-preservation before stabilizing within two months (Figure 5). This trend has been observed by others with evidence that crustaceans reach equilibrium soon after preservation, however medusae and jelly-like constituents take longer to stabilize (Ahlstrom & Thrailkil, 1962; Kapiris *et al.*¸1997). This result highlights the importance of timing scans after all individuals in the sample have stabilized to ensure that no more shrinkage will occur and the conversion factors can be used accurately. If samples were scanned before stabilization, this would likely result in an overestimation of biomass from measurements of zooplankters that have not reached equilibrium shrinkage.

One factor that influenced the results in this study was the loss of individuals over time. Although efforts were made to reduce damage to zooplankton samples during handling and processing, some individuals were still broken and categorized as “damaged”. These damaged zooplankton (ie. with broken legs, shredded carapaces, splitting bodies) likely accounted for the loss of individuals over time as evidence by greater numbers of “damaged” individuals in

preserved than fresh samples, which could bias the results and increase the variability. However, to alleviate the possible effects, clusters of area, biomass, and major/minor lengths were examined over each scan day to identify which individuals had been lost. This further exploration showed that there was an even distribution of large and small individuals lost, thus these losses are unlikely to skew the average biovolume to either side over time.

Although the calculation for biovolume of euphausiids was corrected, it is still an estimate and could be inaccurate due to their curvature. It was also noticed during scanning that the carapace of the euphausiid tended to flip up over time after preservation (Supplementary data, Figure A3), which would skew the biometric measurements with a possible overestimation of biovolume. This may explain the unexpected results seen among the small euphausiids, whereby the average preserved percent biovolume was *greater* than the fresh percent biovolume (Table 2). The inclusion of the flipped-up carapace in biometric measurements may thus explain the unexpected increase in the preserved average percent biovolume.

During the Zooscan scanning procedure, samples were rinsed with freshwater before scanning and placed in freshwater during scanning, which may have also influenced the rate of shrinking after preservation. Omori (1978) found that body substances were rapidly lost after contact with distilled water. Due to the hypotonic nature of distilled water compared to seawater, cells experienced osmotic damage and intracellular material was lost. These effects may be alleviated by rinsing with isotonic ammonium formate instead.

To further improve this study, more taxa could be studied to incorporate more conversion factors. For some taxa, more individuals could be scanned to provide greater precision of the conversion factors. And finally, to ensure that all samples have stabilized, shrinkage could be continually monitored through dispersed scanning over months and possibly years. These suggestions would further develop the ability to estimate biomass through image analysis of zooplankton samples preserved in formalin. A limitation of image analysis however, is that there are restrictions on the extent of taxonomic resolution. Not all developmental stages and species of zooplankton taxa can be identified based on vignettes of individuals without microscopic work.

In conclusion, these conversion factors that have not been previously reported now allow for correction of biovolume estimates that would normally underestimate biomass due to the observed shrinkage in formalin-preserved zooplankton. In addition, this highlights the amount of

bias in biovolume estimates of previous studies. This method also differs from the usual destructive methods involved to estimate biomass, that while functional, do not maintain high taxonomic resolution or provide as many opportunities for future analysis of samples. Therefore, the non-destructive method of image-analysis paired with the acquired conversion factors allow for more accurate biomass estimates that can be applied to preserved historical samples or in ground-truthing observations from bioacoustics. Findings of zooplankton patterns and distributions can then be used to evaluate the survival or growth of higher trophic levels.

ACKNOWLEDGEMENTS

I would first like to thank my supervisor Dr. John Dower for the opportunity to undertake this project, which has cultivated an appreciation and desire to research and learn about the significance of zooplankton in our oceans. I would also like to thank Nic Ens, who spent countless hours supporting me with sample sorting and scanning, as well as providing extensive instruction on coding in R. I am so appreciative of all his support and for the many constructive discussions and edits over the year. The support of Dr. Steve Perlman and Dr. Barbara Hawkins in leading the honors program has been encouraging throughout this experience and is very appreciated. I would also like to extend my thanks to Chelsea Stanley and Stéphane Gauthier at Fisheries and Oceans Canada for their support in sample collection and for providing the opportunity for me to participate in the Hake survey in August 2022. Lastly, I would like to thank my friends and family for the love and support throughout this process. Thank you for listening to my endless rambles about zooplankton in the last year.

REFERENCES

Ahlstrom, E. H. and Thrailkill, J.R. (1963) Plankton volume loss with time of preservation. *Calif. Coop. Oceanic Fish. Invest. Rep.*, **9**, 57-73.

Alcaraz, M., Saiz, E., Calbet, A., Trepat, I., and Broglio, E. (2003) Estimating zooplankton biomass through image analysis. *Marine Biology*, **143**, 307–315.

Benfield, M. C., Wiebe, P. H., Stanton, T. K., Davis, C. S., Gallager, S. M., and Greene, C. H. (1998) Estimating the spatial distribution of zooplankton biomass by combining Video Plankton Recorder and single-frequency acoustic data. *Deep Sea Research Part II: Topical Studies in Oceanography*, **45**, 1175–1199.

Cass, C. J. and Daly, K. L. (2015) Ecological characteristics of eucalanoid copepods of the eastern tropical North Pacific Ocean: Adaptations for life within a low oxygen system. *Journal of Experimental Marine Biology and Ecology*, **468**, 118–129.

Cornils, A., Thomisch, K., Hase, J., Hildebrandt, N., Auel, H., and Niehoff, B. (2022) Testing the usefulness of optical data for zooplankton long-term monitoring: Taxonomic composition, abundance, biomass, and size spectra from ZooScan image analysis. *Limnology & Ocean Methods*, **20**, 428–450.

Cushing, D. H. (1990) Plankton Production and Year-class Strength in Fish Populations: an Update of the Match/Mismatch Hypothesis. *Advances in Marine Biology*. Elsevier, pp. 249–293.

Dai, L., Li, C., Yang, G., and Sun, X. (2016) Zooplankton abundance, biovolume and size spectra at western boundary currents in the subtropical North Pacific during winter 2012. *Journal of Marine Systems*, **155**, 73–83.

Davis, C., Hu, Q., Gallager, S., Tang, X., and Ashjian, C. (2004) Real-time observation of taxa-specific plankton distributions: an optical sampling method. *Mar. Ecol. Prog. Ser.*, **284**, 77–96.

Devi, C.B.L. (1972) Fixation and preservation of plankton samples. Handbook to the International Zooplankton Collections, Vol. 3.

Di Mauro, R., Cepeda, G., Capitanio, F., and Viñas, M. D. (2011) Using ZooImage automated system for the estimation of biovolume of copepods from the northern Argentine Sea. *Journal of Sea Research*, **66**, 69–75.

Garcia-Comas, C. (2010) Short manual to work with the ZooScan. Written for Zooprocess version 6.16. Hydroptic & LOV, 1-15.

Garijo, J. C. and Hernández-León, S. (2015) The use of an image-based approach for the assessment of zooplankton physiological rates: a comparison with enzymatic methods. *J. Plankton Res.*, **37**, 923–938.

Gasparini, S. (2013) Plankton Identifier [Computer software]. BP 28 – 06234 Villefranche sur mer Cedex, France: Laboratoire d'Océeanographie de Villefranche.

Gifford, D. J. and Caron, D. A. (2000) 5 - Sampling, preservation, enumeration and biomass of marine protozooplankton. In Harris, R., Wiebe, P., Lenz, J., Skjoldal, H. R., and Huntley, M. (eds), ICES Zooplankton Methodology Manual. Academic Press, London, pp. 193–221.

Giguère, L. A., St-Pierre, J.-F., Bernier, B., Vézina, A., and Rondeau, j.-G. (1989) Can We Estimate the True Weight of Zooplankton Samples after Chemical Preservation? *Can. J. Fish. Aquat. Sci.*, **46**, 522–527.

Gislason, A. and Silva, T. (2009) Comparison between automated analysis of zooplankton using ZooImage and traditional methodology. *Journal of Plankton Research*, **31**, 1505–1516.

Gorsky, G., Ohman, M. D., Picheral, M., Gasparini, S., Stemmann, L., Romagnan, J.-B., Cawood, A., Pesant, S., *et al.* (2010) Digital zooplankton image analysis using the ZooScan integrated system. *Journal of Plankton Research*, **32**, 285–303.

Hernández-León, S. and Montero, I. (2006) Zooplankton biomass estimated from digitalized images in Antarctic waters: A calibration exercise. *Journal of Geophysical Research: Oceans*, **111**.

Kapiris, K., Miliou, H., and Moraitou-Apostolopoulou, M. (1997) Effects of formaldehyde preservation on biometrical characters, biomass and biochemical composition ofAcartia clausi (Copepoda, Calanoida). *Helgoländer Meeresunters.*, **51**, 95–106.

Lafontaine, Y. D. and Leggett, W. C. (1989) Changes in Size and Weight of Hydromedusae During Formalin Preservation. *Bulletin Of Marine Science*, **44**, 9.

Mayzaud, P., Boutoute, M., and Alonzo, F. (2003) Lipid composition of the euphausiids *Euphausia vallentini* and *Thysanoessa macrura* during summer in the Southern Indian Ocean. *Antartic science*, **15**, 463–475.

McEnnulty, F. R., Davies, C. H., Armstrong, A. O., Atkins, N., Coman, F., Clementson, L., Edgar, S., Eriksen, R. S., et al. (2020) A database of zooplankton biomass in Australian marine waters. *Sci Data*, **7**, 297.

Nakamura, A., Matsuno, K., Abe, Y., Shimada, H., and Yamaguchi, A. (2017) Length-weight Relationships and Chemical Composition of the Dominant Mesozooplankton Taxa/species in the Subarctic Pacific, with Special Reference to the Effect of Lipid Accumulation in Copepoda. *Zool Stud*, **56**, e13.

Omori, M. (1978) Some Factors Affecting on Dry Weight, Organic Weight and Concentrations of Carbon and Nitrogen in Freshly Prepared and in Preserved Zooplankton. *Internationale Revue der gesamten Hydrobiologie und Hydrographie*, **63**, 261–269.

Põllupüü, M. (2007) Effect of formalin preservation on the body length of copepods. *Proc. Estonian Acad. Sci. Biol. Ecol.*, **56**, 326-331.

Rasmussen, J. H., Moyano, M., Fuiman, L. A., and Oomen, R. A. (2022) FishSizer: Software solution for efficiently measuring larval fish size. *Ecology and Evolution*, **12**, e8672.

Stoecker, D., Gifford, D., and Putt, M. (1994) Preservation of marine planktonic ciliates: losses and cell shrinkage during fixation. *Mar. Ecol. Prog. Ser.*, **110**, 293–299.

Thibault-Botha, D. and Bowen, T. (2004) Impact of formalin preservation on *Pleurobrachia bachei* (Ctenophora). *Journal of Experimental Marine Biology and Ecology*, **303**, 11–17.

Wolowicz, M. and Szaniawska, A. (1986) Calorific value, lipid content and radioactivity of common species from Hornsund, southwest Spitsbergen. *Polar Research*, **4**, 79–84.

SUPPLEMENTARY DATA

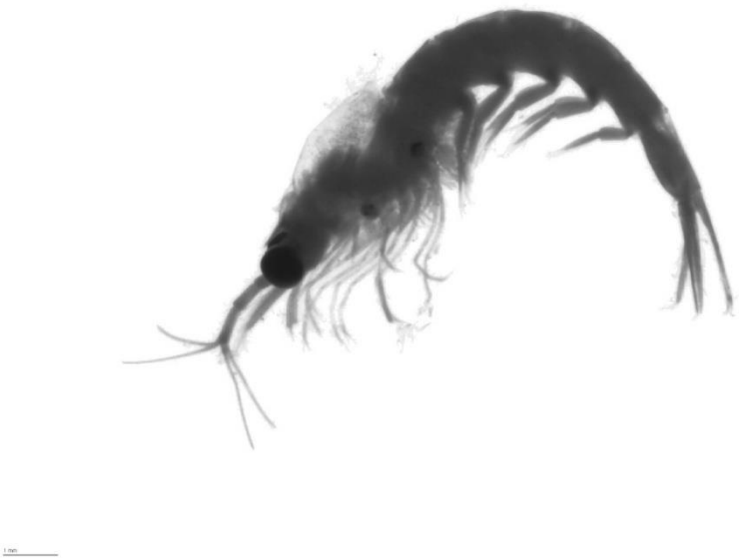

Figure A1. Euphausiid vignette with an estimated biovolume of 70.9407 mm^3 before correction and 12.1441 mm^3 after correction.

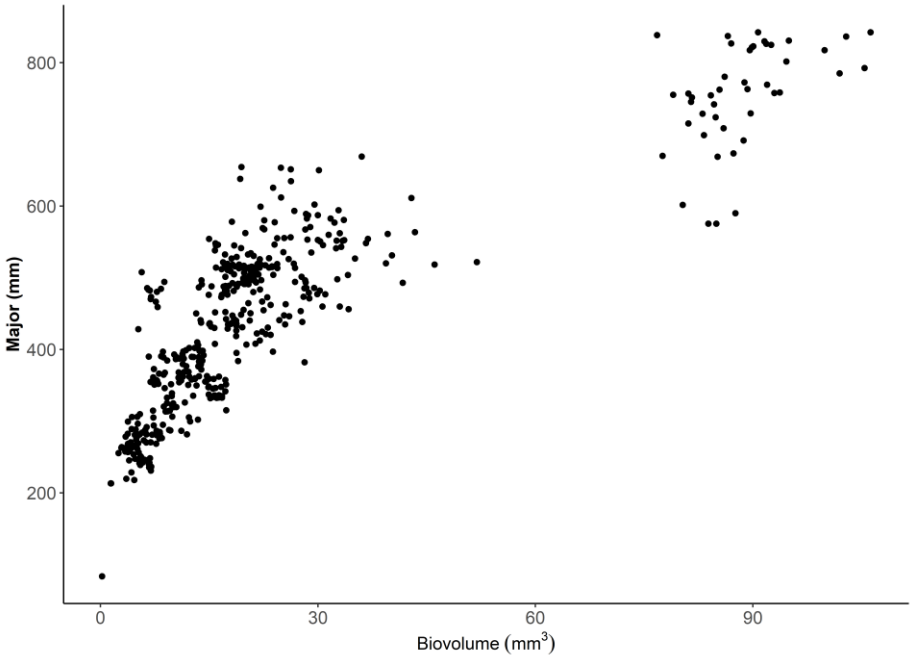

Figure A2. Scatterplot of biovolume (BV) against the major axis used to further divide hyperiid taxa into size categories. Example in figure shows distinct clusters of different sized hyperiids; large individuals defined as BV > 60 mm^3 and small individuals BV < 60 mm^3.

Figure A3. Examples of flipped-up carapaces of euphausiids after 58 days of preservation in buffered formalin solution.